Transilvania University of Brasov,
Romania

13th INTERNATIONAL CONFERENCE
"STANDARDIZATION, PROTYPES AND QUALITY:
A MEANS OF BALKAN COUNTRIES' COLLABORATION"

Brasov, Romania, November 3 - 4, 2016

Accurate Determination of the Thermal Model Time Constant for the Electrical Servomotors

DANILA Adrian
Transilvania University of Brasov, Romania, adrian.danila@unitbv.ro
CAMPEANU Radu
Transilvania University of Brasov, Romania, radu.campeanu@unitbv.ro

Abstract
The thermal model of the electrical drives is used to predict the critical thermal stress of the drive in conjunction with its duty cycle. The accuracy of the predictions based on the simplified thermal models depend on the accuracy of the estimates for the model's parameters. In this work, authors investigated the implementation of the infrared cameras and EDT method for the contactless estimation of the time constant of the thermal model of the electrical machines. In the first and the second chapter of the work, the theoretical background is presented. The main standards related to the problem are revised and the single-body model of the electrical machine is emphasized. In the third and the fourth chapters the experimental implementation and results are presented. The investigation proved that the time-dependency of the maxima temperature, determined with the thermal camera, follows an exponential curve as given in the literature and may be used for the accurate estimation of the time constant of the thermal model of the drive.

Keywords
electrical servomotors, thermal model, time constant, thermal camera

1. Introduction

The duty of an electrical drive defines the dependency of the load power, and thus of the power losses in the machine as function of time. The power losses in the machine determine the increase of the temperature of the active parts of the machine. The weakest part of the electrical machines is the electrical insulation of the windings. Therefore, the heating of the electrical machine is the critical limitation during the drive's operation.

The duties of the electrical drives are defined in the SR EN 60034-1:2005, „Rotating electrical machines - Part 1 Rating and performance". The base duty type is S1 - continuous running type. For electrical servo motors and general purpose electrical machines, the following duty types are defined into the standard: the duty type S2 - short-time duty; the duty type S3 - intermittent periodic duty; the duty type S4 - intermittent periodic duty with starting; the duty type S5 - intermittent periodic duty with electric braking; the duty type S6 - continuous operation periodic duty; the duty type S7- continuous operation periodic duty with electric braking, and the duty type S8 - continuous-operation periodic duty with related load/speed changes.

For each duty type mentioned above, the heating model of the machine may be deduced based on the thermal models of the drive. This is useful at the design stage of the drive, but also during the drive operation for the on-line detection of possible faults. The thermal models of a drive allow predictions over the drive's operation. The accuracy of the predictions is closely related to the correct estimation of the model's parameters. Generally speaking, the determination of the parameters of the electrical machines is well defined and standardized. The standard SR EN 60034-2-1 (CEI 60034-2-1) „Rotating electrical machines - Part 2-1" refers to the standard methods for determining losses and efficiency from tests. The standard CEI 60034-1 at par. 8.6.2.3.3 defines the following methods for the temperature measurements (a) the resistance method (b) embedded temperature detector (ETD) method and (c) thermometer method.

Based on the above standards, the authors of this paper investigated the implementation of the

infrared cameras and EDT method for the estimation of the time constant of the thermal model of the electrical machines.

2. Problem Formulation and Solution

2.1. Thermal models of the electrical machines

The electrical machines are non homogenous, non isotropic, complex systems made of solid and fluid materials with distributed heating sources.

The heat exchange is made by thermal conduction in solid materials, radiation and convection through fluids. The true model of the heat exchange in the electrical machines is depicted by a second order partial differential equation, depicting the thermal diffusion with initial conditions and boundary conditions, depending on the geometrical model of the machine and the thermal transfer conditions.

$$\frac{\partial}{\partial x}\left(\lambda_x \cdot \frac{\partial \Theta}{\partial x}\right)+\frac{\partial}{\partial y}\left(\lambda_y \cdot \frac{\partial \Theta}{\partial y}\right)=-q-c\cdot\rho\cdot\frac{\partial \Theta}{\partial t} \tag{1}$$

where, $\Theta(x;y)$ is the temperature at a given point of the two-dimensions space of the electrical machine; q - is the volume density of power of the heating sources, c - the specific heat, ρ - the density of the materials, λ_x, λ_y - are the components of the thermal conductivity.

The solution of the problem depicted above may be obtained numerically with complex thermal models of the machine and the Finite-Element Method, e.g. the papers [3, 4, 9], or other methods, [10]. Despite the complex implementation, this approach may lead to inaccurate solutions if the thermal constants of the materials are inaccurate, and the distributed parameters problem is not well-posed.

Usually, the electrical machines volume is limited in the 3D space. Therefore, for the practical applications such as the design of electrical drives, simplifications are possible to avoid the complex models.

The following two cases are to be taken into account.

- If the machine has a magnetic circuitry in the induced, then the whole machine may be equivalent with a unique homogenous, isotropic body with the thermal resistance R_ϑ and the thermal capacitance C_ϑ. This approach leads to a thermal model of the machine called the single-body model.
- Thermal constant of the inductor and the induced are different if the induced of the machine is not of magnetic circuitry. In this case, the induced must be considered separately of the inductor and the housing. This approach leads a model of the machine called the two-body model. The two-body model applies to the servo motors with bell-shaped rotors, flat rotors or with resin-consolidated rotors.

2.2. The single-body model of the electrical drives

The differential equation that depicts the thermal process is as follows, [1], [2].

$$P_J(t)=C_\vartheta\cdot\frac{d\vartheta(t)}{dt}+\frac{1}{R_\vartheta}\cdot\left[\vartheta(t)-\vartheta_a\right]\quad \vartheta(0)=\vartheta_i\,, \tag{2}$$

where $P_J(t)$ are the Joule-Lenz power losses, ϑ_a is the ambient temperature and $\vartheta(0)=\vartheta_i$ is the temperature at the initial moment of the process

The resulting transfer function has the following form:

$$G_1(s)=R_\vartheta\cdot\frac{1}{1+s\cdot\tau}\,. \tag{3}$$

The thermal resistance of the machine depends on the shape, materials and dimensions of the machine. The term $\tau=R_\vartheta\cdot C_\vartheta$ is the time constant of the thermal model of the drive. The expression (3) depicts a proportional first-order element.

The general form of the solution of the first order differential equation is the following:

$$\vartheta(t)=\vartheta_f\cdot\left[1-e^{\frac{-t}{\tau}}\right]+\vartheta_i\cdot e^{\frac{-t}{\tau}}+\vartheta_a\,, \tag{4}$$

where ϑ_i and ϑ_f are the initial value and the final value of the over-temperature. At the start-up of the

machine, $\vartheta_i = 0$, thus the heating process is depicted as follows.

$$\vartheta(t) = \vartheta_f \cdot \left[1 - e^{\frac{-t}{\tau}}\right] + \vartheta_a . \tag{5}$$

During the cooling process, $P_J = 0$ and $\vartheta_f = 0$ the cooling process is depicted as follows.

$$\vartheta(t) = \vartheta_i \cdot e^{\frac{-t}{\tau}} + \vartheta_a . \tag{6}$$

The expression above allows estimate the time constant of the thermal model from data either by means of the Strejic method or by the graphical-analytical method described in [5].

3. The Experiment's Organization and Results

3.1. The setup of the experiment

The experiment took place within the context of the studies related to the electronically switched capacitor for the two-phase capacitor-run induction motor. In this context, the aim was the evaluation of the energy efficiency of the drive at various values of the equivalent capacitance of the electronically switched capacitor.

The evaluation of losses and drive efficiency was made according to the SR EN 60034-2-1for the duty type S2, short-time duty, according to the standard SR EN 60034-1:2005 and the embedded temperature detector (EDT) method, [7].

Within the experiment the following time dependencies were measured and recorded: (1) the voltage and current at the terminals of the main winding; (2) the voltage and current at the terminals of the auxiliary winding; (3) the voltage drop at the terminals of the capacitor; (4) the electromagnetic torque at zero angular speed; (5) the increase of the rotor temperature as long as the motor was to the network supply, and (6) the decrease of the rotor temperature as long as the motor was disconnected from the network supply.

The experimental setup is presented in Figures 1 and 2. The servomotor tested was of type MSP 311. The rated parameters of the servomotor are presented in Table 1.

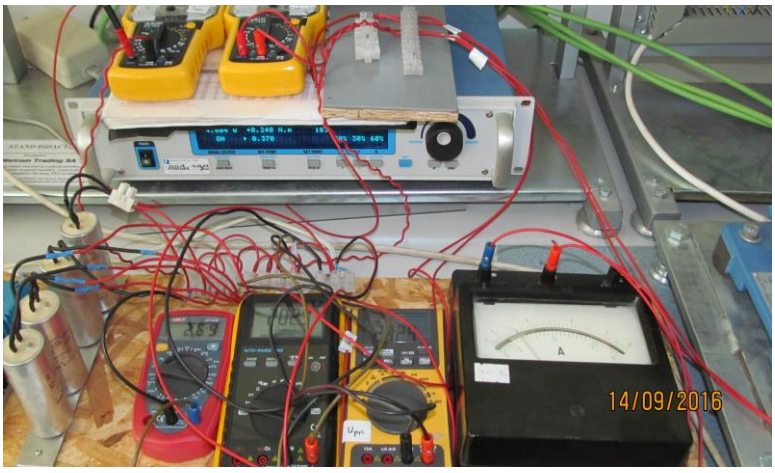

Fig. 1. The experiment setup. The measurement apparatus

Table 1. The rated parameters of the MSP 311 Machine

No.	Denomination	Units	Value
1	Rated Supply Voltage	V	230
2.	Rated Frequency	Hz	50
3.	Rated Speed	rpm	2840 / 420
4	Number of Poles	-	2 / 12
5	Capacitor-Run Rated Capacitance	μF	14

Fig. 2. The thermal camera location with respect to the electrical motor

The rotor of the servomotor was locked by means of a powder brake of type 2 PB 43 (rated torque 10 N·m, rated power 1 kW, rated speed 955 rpm and maximum speed 4000 rpm, and the rated excitation current 2A). The control of the powder brake was made by means of a dynamometer controller of type DSP 6001.

The electrical measurements were performed with electronically voltmeters and amperemeters - with 3.5% accuracy and the appropriate measurement range. The electromagnetic torque was measured by means of the torque transducer, with the signal adapter of type TSC 401/111 attached to the brake, and with the display module of type DSP 6001 - ±0, 5% accuracy. The thermal field of the rotor was evaluated with a thermal camera of type Fluke TiR infrared camera - temperature range from -20 °C to +100 °C and 5% accuracy.

Measured data, acquired from the process was processed by means of the following software applications: (1) an application in the Scilab software environment with the SIVP - Scilab Image and Video Processing Toolbox for the 3D-profile of the thermal field of the rotor, (2) an application, in the Scilab software environment for the estimation of the minimum values, the maximum values, and the average values of the temperature distributions from acquired data, for the graphical representations and for the estimation of the time constant.

The experiments' steps were the followings. (1) The servomotor - the test-unit -, initially at the environmental temperature, had been connected to the supply network. (2) The electrical variables and the mechanical variables were measured and recorded. (3) At equal time intervals a snapshot of the thermal field was recorded. (4) The process continued until the rotor's temperature of the rotor had reached the maximum admissible value. At this moment the electrical variables and the mechanical variables were recorded. (5) The steps (1) to (4) have been repeated for each configuration of the stator windings and four different values of the capacitor-run capacitance.

3.2. The experimental data

The recorded data of the electrical variables and the mechanical variables are presented in Table 2 and in Table 3.

Table 2. The Electrical Variables and the Mechanical Variables;
Servomotor Connected to the Voltage Supply

Denomination	Units	Values						
No. of poles	-	12	12	12	12	2	2	2
Capacitor-Run Capacitance	μF	15	11.25	7.5	3.75	15	11.25	7.5
Total Current	A	1.56	0.95	1.5	1.55	4.4	4.19	3.8
Main Current	A	1.42	1.57	1.66	1.64	3.48	3.78	3.75
Auxiliary Current	A	1	0.71	0.44	0.18	1.27	1.04	0.67
Main Voltage	V	232	229.9	229.9	230.6	228.4	226	226
Auxiliary voltage	V	150	95.2	62.8	53	159.5	126	103
Capacitor voltage drop	V	201	200	191	176	264	289	257
Electromagnet Torque	N·m	0.24	0.177	0.109	0.047	0.115	0.108	0.076
Speed	rpm	0	0	0	0	0	0	0

Table 3. The Electrical Variables and the Mechanical Variables;
Servomotor Disconnected from the Voltage supply

Denomination	Units	Values						
No. of poles	-	12	12	12	12	2	2	2
Capacitor-Run Capacitance	μF	15	11.25	7.5	3.75	15	11.25	7.5
Total Current	A	1.56	0.7	1.28	1.28	4	3.61	3.3
Main Current	A	1.42	1.35	1.39	1.38	3.28	3.21	3.2
Auxiliary Current	A	1	0.7	0.44	0.18	1.25	1.01	0.65
Main Voltage	V	232	228.8	229.9	230.3	223.1	226.8	227
Auxiliary voltage	V	150	110.5	73.5	54.6	161.3	138.3	109
Capacitor voltage drop	V	201	197	191	177	258	281	294
Electromagnet Torque	N·m	0.24	0.177	0.112	0.048	0.111	0.098	0.072
Speed	rpm	0	0	0	0	0	0	0

In Figure 3 a capture of the thermal field at the rotor surface, during the experiment is presented, and in Figure 4, the 3D-profile of the thermal field, computed with the Scilab environment and the SIVP module is depicted.

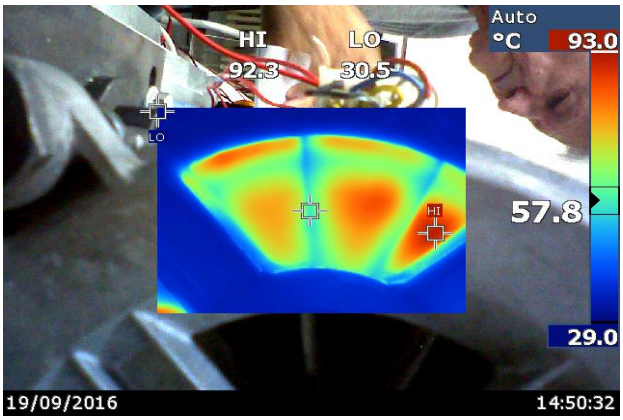

Fig. 3. The capture of the thermal field of the rotor made with the thermal camera during a test

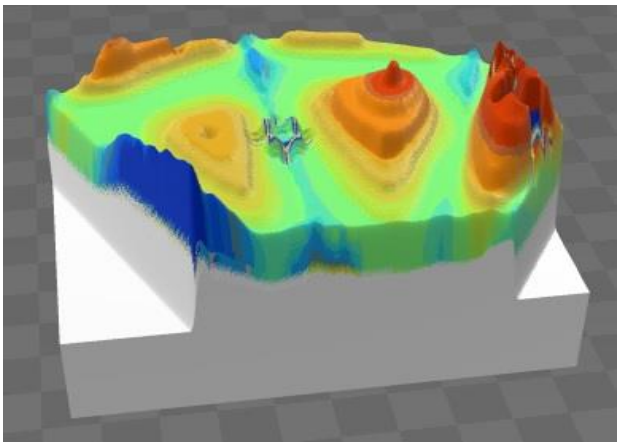

Fig. 4. The 3D-profile of the thermal field of the rotor computed with the image processing application

4. Discussion

The data in Tables 3 and 4 emphasizes that an increase of 70 ^{0}C of the temperature at the rotor surface does not affect significantly the critical electromagnetic torque of the servo motor. This means that the increase of the equivalent resistance of the rotor with temperature may be neglected, in this experiment.

The estimates of the thermal field temperatures, minima and maxima on the rotor's cross-section are depicted in Figures 5 and 6. The highest value of the temperature is reached at the rotor's surface, within the air gap and is due to the Joule-Lenz effect of the induced currents. The lowest value of the temperature occurs near the shaft of the machine and varies due to the thermal diffusion from the surface through the rotor's body.

The average estimate of the temperature distribution on the rotor cross section is also depicted in Figures 5 and 6. Although, usually, average decreases noise effects, in this case the estimates are still disturbed by noise.

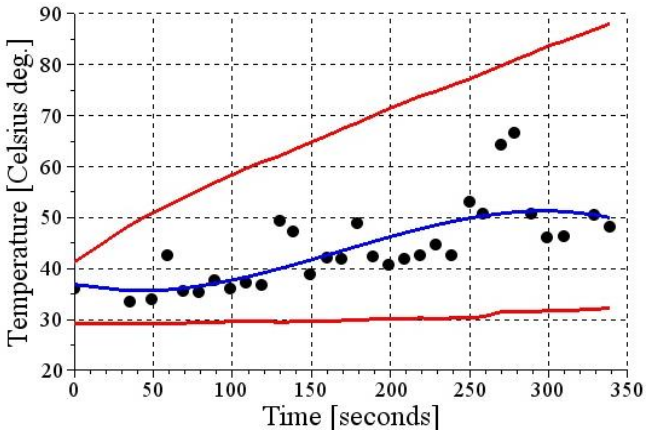

Fig. 5. The average measured temperatures during the heating process: the upper and the lower red lines represent the maximum and minimum values respectively. The dots represent the estimated equivalent temperature of the rotor, and the central blue line represents the least-squares approximation curve of the estimated equivalent temperature of the rotor

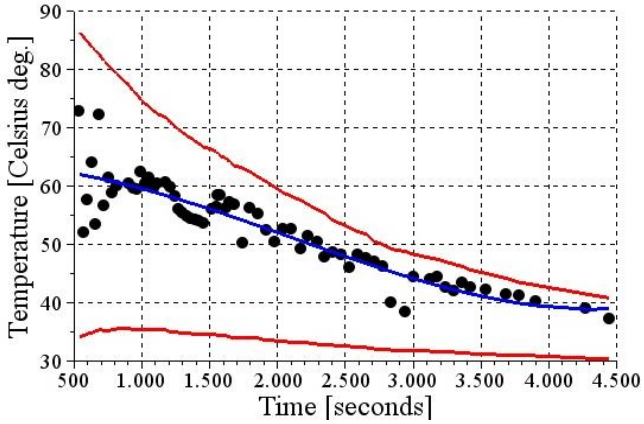

Fig. 6. The average measured temperatures during the cooling process: the upper and the lower red lines represent the maximum and minimum values, respectively. The dots represent the estimated equivalent temperature of the rotor, and the central blue line represents the least-squares approximation curve of the estimated equivalent temperature of the rotor

This is due to the fact that large areas that do not occur to the heating process are introduced in computations. To avoid this, the area of interest must be restricted to the area near by the rotor's surface.

Figure 6 depicts the cooling process of the rotor. The time-dependency of the maxima temperature follows an exponential curve as depicted in the expressions (5) and (6). This curve allows the estimation of the time constant either by means of the Strejic empirical method or by the graphical-analytic method described in [5].

This dependency is similar to the time dependency of the speed in the free-braking test for the inertia axial moment of the drive.

References

1. Grellet, G., Clerc, G. (2000): *Actionneurs Electriques Principes / Modèles / Commande* Éditions. Eyrolles, ISBN 2-212-09352-7 Paris, p. 122-140 (in French)
2. Saal, C., Topa, I., Fransua, Al., Micu, E. (1980): *Acţionări electrice şi automatizări* (*Electrical Drives and Automations*). Editura Didactică şi Pedagogică, Bucureşti, p. 233-240 (in Romanian)
3. Dorell, D.A. (2008): *Combined Thermal and Electromagnetic Analysis of Permanent-Magnet and Induction Machines to Aid Calculation*, IEEE Transactions on Industrial Electronics, ISSN 1557-9948, Vol. 55, no. 10, p. 3566-3574
4. Danila, A. (1980): *Experimental Identification and Accurate Model Validation of the Thermal Model of an Electric Machine Based on the Finite Elements Method*. Proceedings of 16th International Conference on System Theory, Control and Computing - ICSTCC, Joint Conference SINTES 16, SACCS 12, SIMSIS 16, p. 1-6, ISBN 978-606-8348-48-3, Sinaia, Romania
5. Danilă, A. (2013): *Modelarea şi identificarea sistemelor dinamice* (*Modelling and identification of dynamic systems*). Editura Universităţii Transilvania din Braşov, ISBN 978-606-19-0271-2, Braşov, p. 8-11 (in Romanian)
6. Dănilă, A., Câmpeanu, R. (2015): *The Implementation of the Frequency Analyzer Principle for the Estimation of the Electronically Switched Capacitor's Capacitance*, RECENT, ISSN 1582-0246, Vol. 16, no. 3(46), p. 216-220, Transilvania University of Brasov, Romania
7. Organismul Naţional de Standardizare din România - ASRO (2005): *SR EN 60034-1:2005. Rotating electrical machines - Part 1 Rating and performance*
8. Organismul Naţional de Standardizare din România - ASRO (2009): *SR EN 60034-2-1 (CEI 60034-2-1). Rotating electrical machines - Part 2-1 standard methods for determining losses and efficiency from tests (excluding machines for traction vehicles)*
9. Zhang, Y., Ruan, J., Huang, T., Yang, X., Zhu, H., Yang, G. (2012): *Calculation of Temperature Rise in Air-cooled Induction Motors Through 3-D Coupled Electromagnetic Fluid-Dynamical and Thermal Finite-Element Analysis*. IEEE Transactions on Magnetics, Vol. 48, No. 2, p. 1047-1050, DOI:10.1109/TMAG.2011.2174433
10. Demetriades, G., De La Para, H.Z., Andersson, E., Olsson, H. (2010): *A Real-Time Thermal Model of a Permanent-Magnet Synchronous Motor*. IEEE Transactions on Power Electronics, Vol. 25, No. 2, p. 463-474, DOI: 10.1109/TPEL.2009.2027905